sci
where science meets business
www.soci.org

Spatial and temporal evolution of the photoinitiation rate for thick polymer systems illuminated by polychromatic light: selection of efficient photoinitiators for LED or mercury lamps

Nicole Stephenson Kenning, Beth A Ficek, Cindy C Hoppe and Alec B Scranton*
Department of Chemical and Biochemical Engineering, University of Iowa, 4133 SC, Iowa City, IA 52242, USA

Abstract

BACKGROUND: Four common free radical photoinitiators were evaluated for use in thick photopolymerizations illuminated with a medium-pressure 200 W mercury–xenon arc lamp and a high-intensity 400 nm light-emitting diode (LED) lamp. For each photoinitiator/lamp combination, the spatial and temporal evolution of the photoinitiation rate profile was analyzed by solving the set of differential equations that govern the light intensity gradient and initiator concentration gradient for polychromatic illumination.

RESULTS: The simulation results revealed that two of the four photoinitiators evaluated were ineffective for photoinitiating thick polymer systems. The photoinitiator bis(2,4,6-trimethylbenzoyl)-phenylphosphine oxide, in combination with the 400 nm LED lamp, was shown to be the most efficient photoinitiator/light source combination for photoinitiation of thick systems.

CONCLUSION: The results show that some photoinitiators commonly used for photopolymerization of thin coatings are ineffective for curing thick systems. LED light sources provide advantages over traditional mercury lamps, and may have tremendous potential in the effective photoinitiation of thick polymer systems.
© 2008 Society of Chemical Industry

Keywords: photoinitiation; photopolymerization; LED; thick polymers

INTRODUCTION

Light-induced polymerization of thick systems (of the order of 1 cm) is relatively uncommon due to issues associated with the optical attenuation of light with increasing sample depth. However, a number of investigators have reported that efficient photopolymerization of thick polymers is possible if the initiating wavelength and initiator systems are chosen carefully to allow sufficient penetration of light through the thickness of the sample.[1–3] It is imperative to avoid initiating wavelengths that are absorbed by the monomer or additives such as fillers or UV stabilizers. In addition, proper pairing of the lamp and the photoinitiator is considerably more complex than in thin systems in which it is only necessary to ensure that the initiator absorbs at the prominent emission wavelengths. For thick systems, the polymerization is inefficient if the molar absorptivity is too high, and an intermediate absorptivity is generally optimal. Even if the system is well designed, the initiation rate in thick systems is highly non-uniform and resembles an initiation wave front that moves from the illuminated surface through the depth of the sample.[4–9] Variables such as initiator concentration, initiator molar absorptivity, initiator photolysis product and incident light intensity have all been shown to affect the height and breadth of this initiation front. Consequently, a fundamental understanding of how a host of variables affect the initiation behavior is needed in order to effectively design reaction systems.

In a previous contribution, a mathematical model was presented to describe the evolution of the photoinitiation rate profile for thick photopolymerization systems illuminated with polychromatic light.[10] This analysis, which is based upon a numerical solution to the governing set of coupled differential equations, provided the first fundamental description of photoinitiation in thick systems for initiators which may photobleach to any extent at each wavelength of illumination. Using representative values of absorption parameters and light-intensity profiles, the complex effects of polychromatic illumination on the resulting photoinitiation rate profile were investigated. It was

* Correspondence to: Alec B Scranton, Department of Chemical and Biochemical Engineering, University of Iowa, 4133 SC, Iowa City, IA 52242, USA
E-mail: alec-scranton@uiowa.edu
(*Received 24 April 2008; revised version received 13 June 2008; accepted 14 June 2008*)
Published online 1 August 2008; DOI: 10.1002/pi.2455

© 2008 Society of Chemical Industry. *Polym Int* 0959–8103/2008/$30.00

demonstrated that for photoinitiation of thick systems with polychromatic light, the shape and attributes of the photoinitiation rate profile change markedly if any of a number of variables are changed, including the relative intensities, absolute intensity, initiator concentration, degree of photobleaching, etc. To optimize the selection of monomers, initiators and light sources for thick photopolymerization systems, it is important to understand and consider all these effects.

In this contribution, the time evolution of the photoinitiation rate profiles for several specific photoinitiator/light source combinations is analyzed and compared using the previously developed approach. Four common photoinitiators which exhibit different photobleaching/photodarkening characteristics are investigated for their efficiency for polymerizing thick systems when illuminated by a standard medium-pressure 200 W mercury–xenon (Hg–Xe) arc lamp. This analysis illustrates that initiator selection rules that may apply for photoinitiation of films and coatings may not be appropriate for thick systems.

Light-emitting diode (LED) light sources offer a number of advantages over traditional mercury lamps, including high energy efficiency, long lamp lifetimes, low heat generation and the absence of hazardous vapors. In addition, LEDs can be instantly switched on and off, are compact and can be tailored to fit a variety of geometric configurations. For example, LED curing units have been shown to be attractive for photocuring dental composites.[11–13] Photoinitiation rate profiles for systems initiated using an LED lamp that emits a high-intensity band at 400 ± 20 nm are compared to those obtained using the 200 W Hg–Xe arc lamp. This study demonstrates that the choice of photoinitiator and light source combination is a complex process that is critical to the success of the photoinitiation.

METHODS

Governing differential equations for polychromatic illumination model

For a thick polymerization system (e.g. 1 cm thick) of rectangular cross-section subject to uniform polychromatic illumination normal to the top surface, the set of differential equations that govern the evolution of the light intensity gradient and initiator concentration gradient for polychromatic illumination are as follows:

$$\frac{\partial C_{\mathrm{i}}(z,t)}{\partial t} = -\frac{C_{\mathrm{i}}(z,t)}{N_{\mathrm{A}}h}\sum_j\left(\frac{\varepsilon_{\mathrm{i}j}\varphi_{\mathrm{i}}I_j(z,t)}{v_j}\right) + D_{\mathrm{i}}\frac{\partial^2 C_{\mathrm{i}}(z,t)}{\partial z^2} \quad (1)$$

$$\frac{\partial C_{\mathrm{p}}(z,t)}{\partial t} = -\frac{C_{\mathrm{i}}(z,t)}{N_{\mathrm{A}}h}\sum_j\left(\frac{\varepsilon_{\mathrm{i}j}\varphi_{\mathrm{i}}I_j(z,t)}{v_j}\right) + D_{\mathrm{p}}\frac{\partial^2 C_{\mathrm{p}}(z,t)}{\partial z^2} \quad (2)$$

$$\frac{\partial I_j(z,t)}{\partial z} = -[\varepsilon_{\mathrm{i}j}C_{\mathrm{i}}(z,t) + A_{\mathrm{m}j} + \varepsilon_{\mathrm{p}j}C_{\mathrm{p}}(z,t)]I_j \quad (3)$$

Here, the subscript j is an index with a different value for each wavelength of light under consideration; $C_i(z,t)$ is the initiator molar concentration at depth z and time t; $C_{\mathrm{p}}(z,t)$ is the photolysis product molar concentration at depth z and time t; $I(z,t)$ is the incident light intensity of a specific wavelength at depth z and time t with units of energy/(area × time); ε_{i} is the initiator Napierian molar absorptivity of a specific wavelength with units of volume/(length × mole); ε_{p} is the photolysis product Napierian molar absorptivity of a specific wavelength with units of volume/(length × mole); φ_{i} is the quantum yield of the initiator at a specific wavelength, defined as the fraction of absorbed photons that lead to fragmentation of the initiator; N_{A} is Avogadro's number; h is Planck's constant; v is the frequency of light in units of inverse seconds; D_{i} is the diffusion coefficient of the initiator in units of (length)^2/time; D_{p} is the diffusion coefficient of the photolysis products; and A_{m} is the absorption coefficient of the monomer and the polymer repeat unit with units of inverse length. Note that this is the Napierian molar absorptivity because it is most natural for the differential version of the absorption equation (Eqn (3)). In the literature the decadic (base 10) molar absorptivity is commonly reported and should be converted to the Napierian value before being used in the model.

The following initial and boundary conditions apply to this system:

$$C_{\mathrm{i}}(z,0) = C_0 \quad (4)$$

$$C_{\mathrm{p}}(z,0) = 0 \quad (5)$$

$$\frac{\partial C_{\mathrm{i,p}}}{\partial z} = 0 \text{ at } z = 0 \text{ and } z = z_{\max} \quad (6)$$

$$I(0,t) = I_0 \quad (7)$$

Equation (4) states that the initial initiator concentration is uniform throughout the depth of the sample. Similarly, Eqn (5) indicates that the initial photolysis product concentration is zero. Equation (6) is the no-flux boundary condition indicating that there is no diffusion through the ends of the sample, and Eqn (7) states that, at any time, the intensity on the surface of the sample where the light enters is equal to the initial intensity of the light source.

The rate of production of free radicals as a function of depth was also considered in this study and is defined by

$$R_{\mathrm{i}}(z,t) = 2C_{\mathrm{i}}(z,t)\sum_j[I(z,t)]_j\phi_j\varepsilon_{\mathrm{i}j} \quad (8)$$

This defines the instantaneous local rate of production of free radicals, $R_{\mathrm{i}}(z,t)$, if two active centers are produced upon fragmentation of the initiator.

The solution to this set of equations provides detailed information regarding the time evolution of the light intensity gradient, the initiator concentration gradient and the photoinitiation rate profile (rate of active center generation as a function of time and location). Once free radical active centers are generated, the subsequent reaction events, such as propagation, termination and chain transfer, are the same for either thick or thin polymerization systems and have been extensively investigated and reported in the literature.[14–16]

For an accurate description of initiation with polychromatic illumination, the light intensity gradient at each incident wavelength must be individually described. As shown by Eqn (3), the intensity of an individual wavelength is attenuated by absorption of the initiator, monomer and polymer repeat units, and the photolysis product. Since the local initiator concentration depends upon all of the incident wavelengths, and the local light intensity of each wavelength depends upon the initiator concentration, the time evolution of all of the light intensities are coupled to one another, and therefore the complete set of differential equations must be solved simultaneously. Therefore, the wavelength dependence of the intensity contributes considerably to the complexity of the model. For a description of n wavelengths of incident light, $n + 2$ equations must be solved simultaneously; typically a 100 nm region of the spectrum is important, so in excess of 100 equations must be simultaneously solved. Previous investigators[8] have shown that diffusion effects will be small for the relatively low initiator concentrations considered in this study, and therefore the diffusion terms were neglected.

Photoinitiators and light sources

Using the approach described above, the photoinitiation rate profiles associated with four commercially available photoinitiators and two common light sources were compared. The photoinitiators were: bis(2,4,6-trimethylbenzoyl)-phenylphosphine oxide (BAPO), 2-benzyl-2-(dimethylamino)-1-[4-(4-morpholinyl)phenyl]-1-butanone (BDMB), 2,2-dimethoxy-2-phenylacetophenone (DMPA) and diphenyl(2,4,6-trimethylbenzoyl)-phosphine oxide (TPO). The first three were obtained from Ciba Specialty Chemicals and the fourth obtained from BASF. These photoinitiators are commonly known to exhibit photobleaching characteristics. The molar absorptivities of all four initiators were determined at concentrations of 0.0268 mol L^{-1} in 1 nm increments using an Agilent UV-visible spectrometer. The wavelengths of interest range from 300 nm (wavelengths below this value are generally unavailable for photoinitiation due to monomer absorption) to approximately 500 nm (above this value, the photoinitiators exhibit no absorption). Figure 1 illustrates the molar absorptivity of each photoinitiator in this spectral region. For each initiator, a typical value for the quantum yield of 0.2 was used. The absorption spectra for each photoinitiator and the corresponding photolysis products were collected using an 8453 UV-visible spectrometer (Agilent Technologies). For these experiments, a 0.01 wt% solution of each photoinitiator in methanol was placed in an air-tight, quartz cell to prevent any changes in concentration due to evaporation of the solvent. To obtain the absorption spectra after photolysis, the samples were illuminated with a 200 W Hg–Xe arc lamp until there was no change in the absorption spectrum.

Two common lamps were used in these studies: a medium-pressure 200 W Hg–Xe arc lamp (Oriel Light Sources) and a high-intensity RX Firefly LED lamp, with emission centered at 400 nm (Phoseon Technology). The relative emission intensities of the lamps were determined at 1 nm increments using an Ocean Optics spectrometer, and the resulting normalized emission spectra are shown in Fig. 2. In this figure, the normalized intensity is defined as the

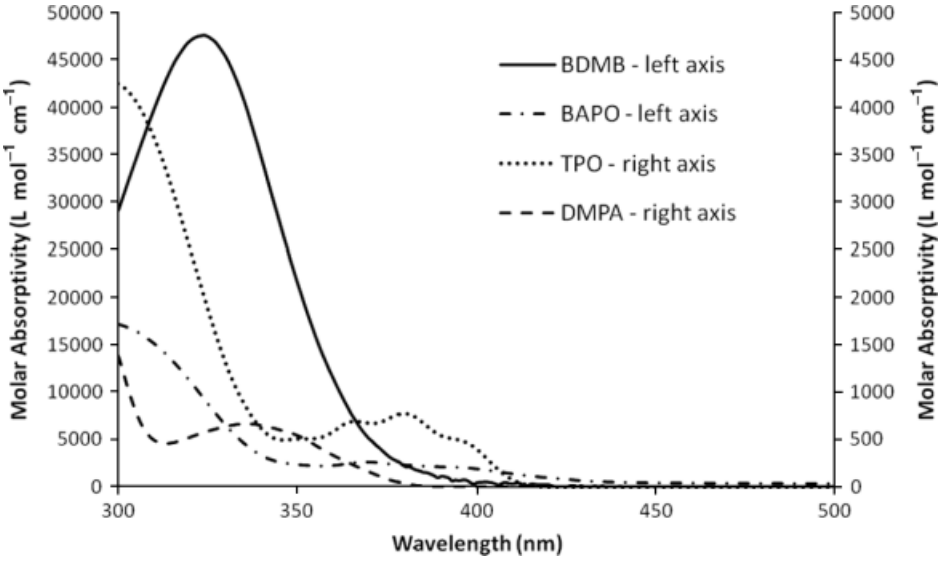

Figure 1. Napierian molar absorptivity *versus* wavelength for the photoinitiators examined.

Polym Int **57**:1134–1140 (2008)
DOI: 10.1002/pi

intensity at the wavelength of interest divided by the total intensity in the 300–500 nm region. The figure illustrates that the Hg–Xe light source has several emission peaks throughout the range of interest, while the LED source has a single large peak centered at 400 nm. The overall intensity of the LED lamp was measured using a black graphite disk in a differential scanning calorimeter, and was found to be 94 mW cm^{-2}. The Hg–Xe lamp has significant emission outside of the wavelengths of interest (300–500 nm); therefore, the relevant intensity of this lamp was obtained by passing the output from the lamp through a 300 nm bandpass filter to remove deep UV radiation and a water filter to remove infrared radiation. To focus this modeling study on the impact of the shapes of the emission spectra rather than the absolute intensity, a total intensity of 94 mW cm^{-2}, which is typical for both lamps in the relevant wavelength range, was used for all simulations.

RESULTS AND DISCUSSION

Comparison of photoinitiators

Choosing the right photoinitiator is critical for an effective cure of a thick polymer system. Since the photoinitiation rate is influenced by many factors all working simultaneously, the choice cannot be based upon a single criterion. For example, inspection of the absorption spectra shown in Fig. 1 reveals that BDMB has extremely high molar absorptivity at the prominent emission wavelengths of the Hg–Xe lamp, suggesting that this initiator may be very attractive for cure with this lamp. While a high molar absorptivity is generally advantageous for photoinitiation in thin systems, other factors in addition to initiator absorptivity must be considered for thick polymer systems, as the simulation results will show.

Simulation results for a thick monomer sample containing 0.0268 mol L^{-1} BDMB illuminated by a 200 W Hg–Xe arc lamp are shown in Fig. 3. Profiles of the photoinitiation rate as a function of depth at four different illumination times are shown. These results illustrate that, immediately upon illumination, the photoinitiation rate at the surface is high, but falls off rapidly with increasing depth due to the high molar absorptivity at the initiating wavelengths. For depths greater than 0.1 cm, the photoinitiation rate is negligible. As the time is increased to 10, 30 and 50 s, the photoinitiation rate throughout the sample decreases with time. Clearly these results illustrate that BDMB is not a suitable choice as a photoinitiator for thick systems.

The time evolution of the photoinitiation rate profile illustrated in Fig. 3 can be explained by comparing the absorption spectrum of the BDMB photolysis products to that of BDMB (Fig. 4). It can be seen that, although the BDMB photoinitiator system exhibits some photobleaching upon photolysis, the molar absorptivity of the photolysis products is still significant (ranging from 22 400 L mol^{-1} cm^{-1} at 320 nm to 2200 L mol^{-1} cm^{-1} at 370 nm), and therefore prevents light penetration into the sample. For this photoinitiator system, the degree of photobleaching is not sufficient to produce a

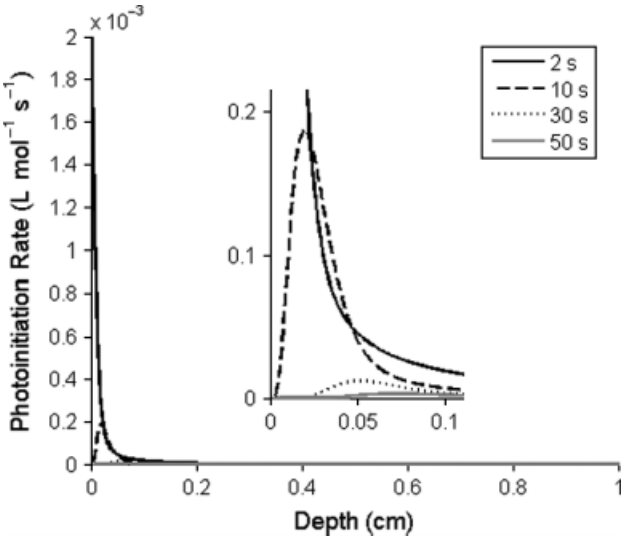

Figure 3. Photoinitiation of a system initiated with BDMB using a medium-pressure 200 W Hg–Xe arc lamp with $I_0 = 94$ mW cm^{-2} and $C_0 = 0.0268$ mol L^{-1}.

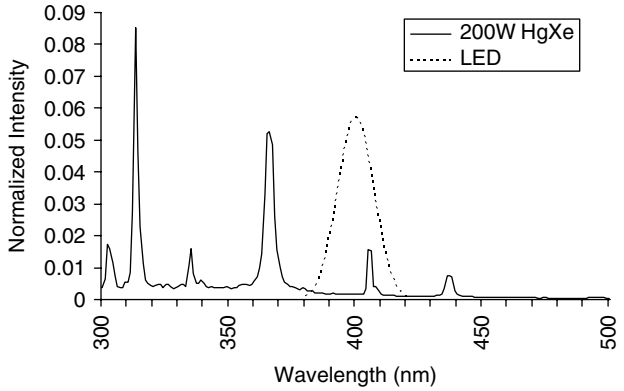

Figure 2. Emission spectra of a 200 W Hg–Xe arc lamp and a high-intensity 400 nm LED lamp.

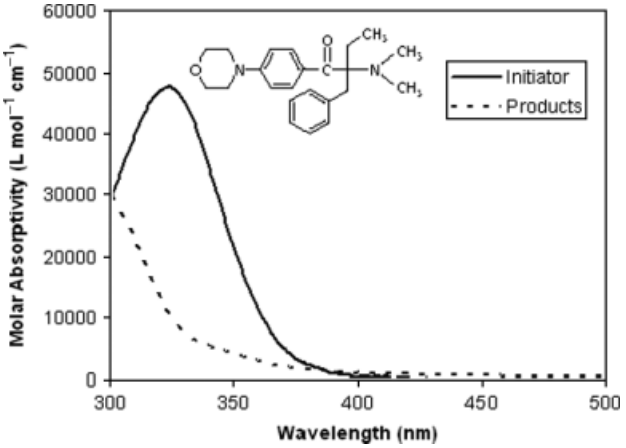

Figure 4. Napierian molar absorptivities of BDMB photoinitiator and respective photolysis products.

photoinitiation wave front that moves into the depth of the sample.

Simulation results for BAPO and TPO, shown in Figs 5(a) and (b), illustrate that these photoinitiators lead to a photoinitiation front that moves through the sample as the illumination time progresses. The photoinitiation wave front peak reaches a distance of 0.32 cm from the illuminated surface after 50 s for the BAPO case and 0.4 cm for the TPO case (recall that for BDMB the photoinitiation rate was essentially zero throughout the sample at 50 s). Figures 6(a) and (b) show the absorption spectra of the BAPO and TPO photolysis products, and illustrate that these initiators exhibit a higher degree of photobleaching than BDMB. This allows the light to penetrate into the thick system as the photoinitiator is consumed near the illuminated surface. The peak of the photoinitiation wave front occurs at the depth for which the product of the incident light intensities and the photoinitiator concentration is maximum.[10] With increasing illumination time, the magnitude of the peak decreases since the photoinitiators do not photobleach completely.

Comparison of the profiles in Fig. 5(a) with those in Fig. 5(b) reveals that the photoinitiation wave fronts produced from BAPO and TPO have considerably different characteristics. The photoinitiation fronts produced by BAPO are sharper (higher in intensity and narrower) and progress through the sample at a lower rate than those produced by TPO. These differences can be attributed to the higher molar absorptivity of BAPO as compared with TPO, as shown in Figs 6(a) and (b). TPO exhibits a lower initiator absorptivity which reduces the photoinitiation rate, but leads to a much broader wave front that moves through the sample more quickly than that of BAPO. BAPO has a much sharper wave front with a higher photoinitiation rate, but penetrates into the sample more slowly. Which photoinitiator is more efficient to use depends on the application.

DMPA is a common photoinitiator for polymerization of films and coatings. Simulation results for photopolymerization of thick systems using this initiator are shown in Fig. 7 for illumination with the Hg–Xe arc lamp. It can be seen that, in this case, there is no photoinitiation rate front that moves through the depth of the sample. The maximum photoinitiation rate remains at or near the illuminated surface for an extended period of time, and the photoinitiation rate is negligible at all times for most of the sample

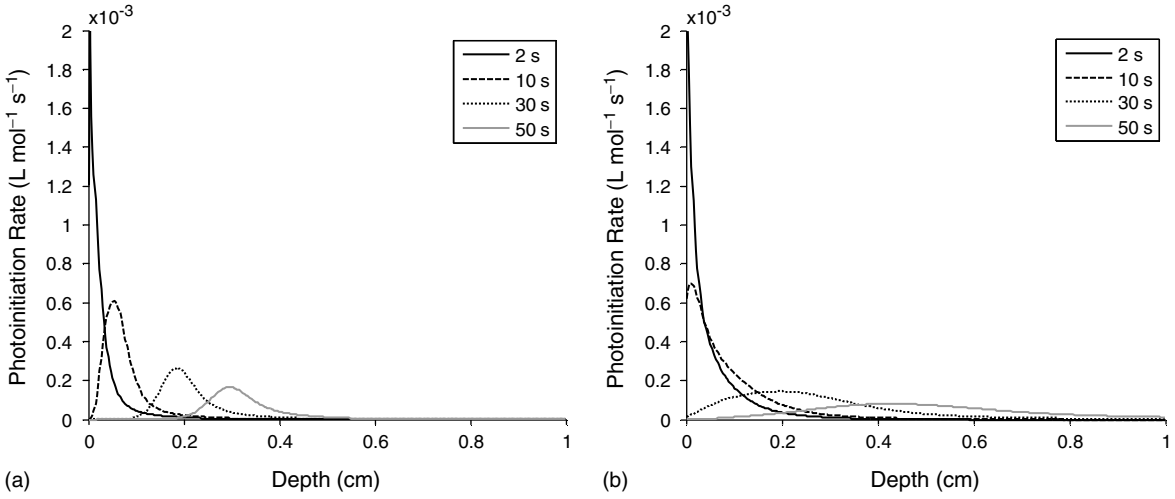

Figure 5. Photoinitiation of a system initiated with (a) BAPO and (b) TPO using a medium-pressure 200 W Hg–Xe arc lamp with $I_0 = 94\,\text{mW cm}^{-2}$ and $C_0 = 0.0268\,\text{mol L}^{-1}$.

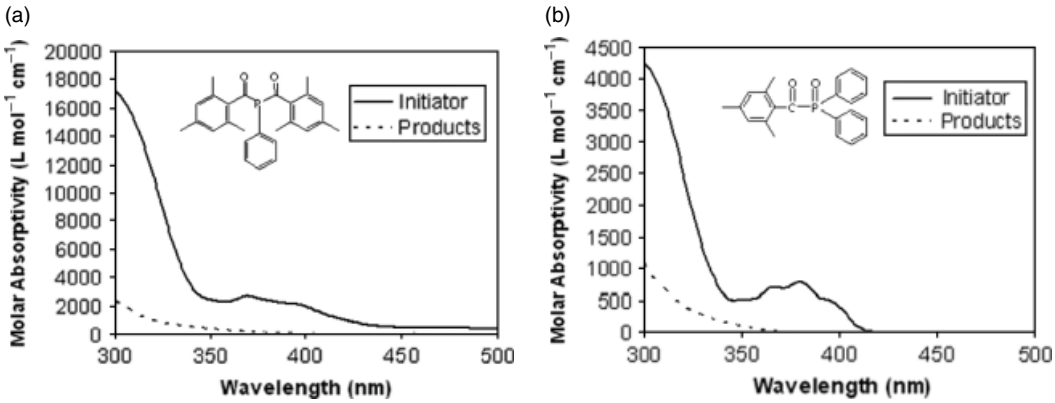

Figure 6. Napierian molar absorptivities of (a) BAPO and (b) TPO photoinitiators and respective photolysis products.

Polym Int **57**:1134–1140 (2008)
DOI: 10.1002/pi

depth. The reason for the lack of deep cure with this initiator is explained by examination of the photolysis product absorption spectrum, shown in Fig. 8. The figure illustrates that although DMPA does absorb in the major peak emission range of the Hg–Xe light source (320–370 nm), the photolysis products also absorb in this region. In fact, the photolysis products exhibit even higher absorbance than the original initiator (photodarkening) in the 300–340 nm range. Due to this competing absorption, light is never able to penetrate deeply in the sample. These results show that examination of the photoinitiator and photolysis product spectra along with the light emission spectrum is imperative for identifying a photoinitiator that will lead to efficient cure of thick polymer systems.

Comparison of light sources

To investigate the potential of thick cure using a commercially available 400 nm LED lamp, the corresponding photoinitiation rate profiles were generated and compared with those for the Hg–Xe lamp. The simulation results for the LED lamp illustrate that BDMB and DPMA are not effective initiators for thick systems for the same reasons that they are ineffective with the Hg–Xe lamp; therefore these results are not presented. In contrast, the LED simulations for BAPO and TPO reveal some interesting, and non-obvious results.

The photoinitiation rate profiles for the sample illuminated with the LED lamp and initiated using BAPO are shown in Fig. 9. It can be seen that the photoinitiation rate profiles for this initiator/lamp combination exhibit higher maximum rates, are more symmetric and move through the sample faster than the corresponding profiles for the Hg–Xe lamp (Fig. 5(a)). These trends arise from the combination of the emission spectrum of the lamp and the absorption spectrum of the initiator. The LED emission spectrum is considerably narrower than that of the Hg–Xe lamp, and lies predominantly in the 390–410 nm range. In this region of the spectrum, the BAPO molar absorptivity is relatively constant, thereby leading to the symmetric photoinitiation rate profile. In contrast, the wide variation in the molar absorptivity in the wavelengths emitted by the Hg–Xe lamp leads to an asymmetric profile in which wavelengths of relatively low molar absorptivity lead to an enhanced photoinitiation rate on the leading edge of the photoinitiation front.[10] The increased maximum photoinitiation rate and enhanced progression of the photoinitiation profile through the sample both arise primarily from the greater extent of photobleaching exhibited by BAPO in the wavelength region emitted by the LED lamp. Figure 6(a) illustrates that BAPO exhibits nearly complete photobleaching in the 390–410 nm range, and therefore essentially all of the incident photons are effective for producing active centers. In contrast, BAPO exhibits incomplete photobleaching for the prominent Hg–Xe emission peaks below 350 nm.

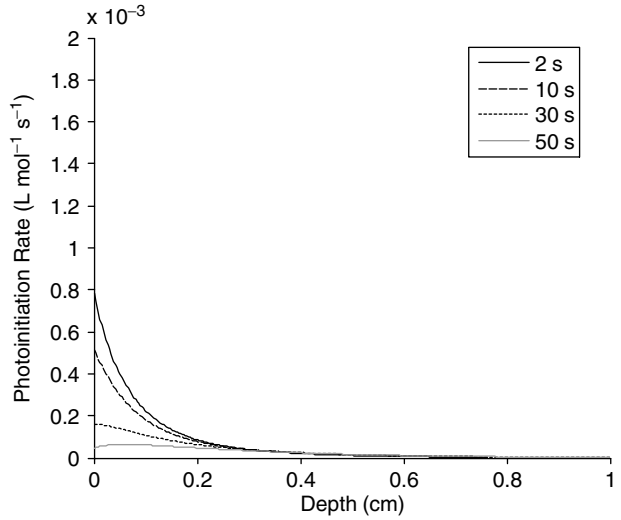

Figure 7. Photoinitiation of a system initiated with DMPA using a medium-pressure 200 W Hg–Xe arc lamp with $I_0 = 94\,\text{mW cm}^{-2}$ and $C_0 = 0.0268\,\text{mol L}^{-1}$.

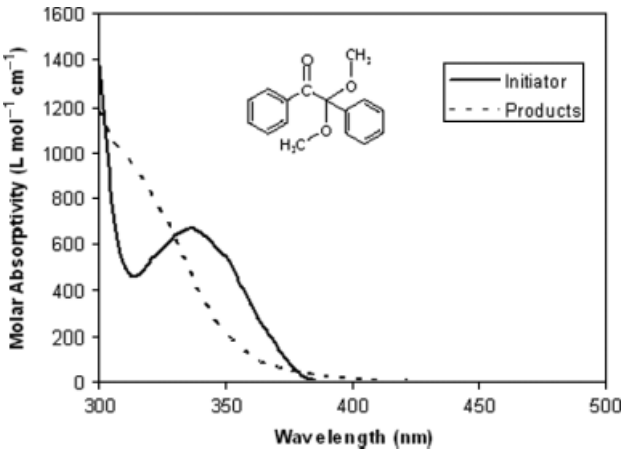

Figure 8. Napierian molar absorptivities of DMPA photoinitiator and respective photolysis products.

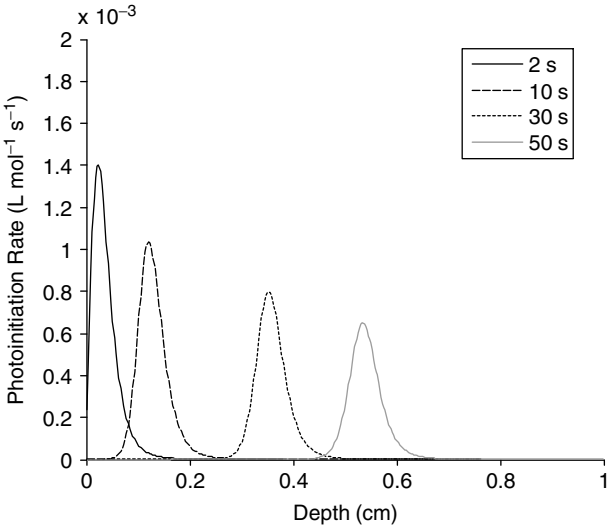

Figure 9. Photoinitiation of a system initiated with BAPO using an LED light source with $I_0 = 94\,\text{mW mm}^{-2}$ and $C_0 = 0.0268\,\text{mol L}^{-1}$.

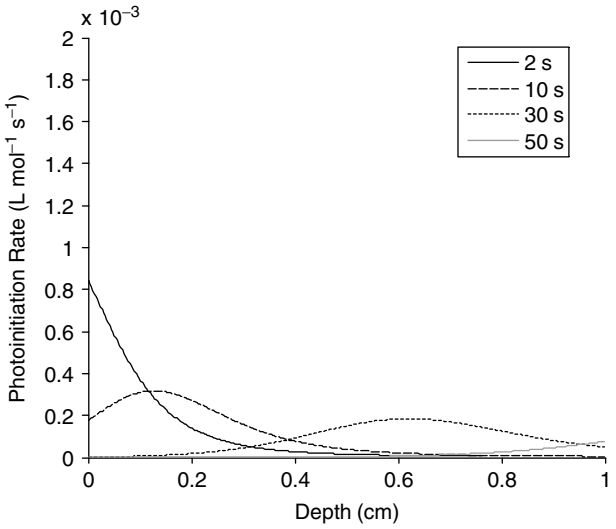

Figure 10. Photoinitiation of a system initiated with TPO using an LED light source with $I_0 = 94\,\text{mW mm}^{-2}$ and $C_0 = 0.0268\,\text{mol L}^{-1}$.

The photoinitiation rate profiles for the sample illuminated with the LED lamp and initiated using TPO are shown in Fig. 10. Comparison of Figs 10 and 5(b) reveals that the LED lamp again leads to an increased maximum photoinitiation rate and a more rapid progression through the sample. Indeed, the maximum rate after 50 s of illumination has moved through the entire depth of the sample in the system illuminated with the LED lamp, while it is only at a depth of 0.42 cm into the sample in the system illuminated with the Hg–Xe lamp. Again, these trends can be explained by the enhanced extent of photobleaching exhibited by TPO in the wavelengths emitted by the LED lamp. As with the Hg–Xe lamp results, the photoinitiation fronts produced by BAPO are sharper (higher in intensity and narrower) than those produced by TPO, due to the higher molar absorptivity of BAPO as compared with TPO in Figs 6(a) and (b).

CONCLUSIONS

In this contribution, the efficiency of four common photoinitiators (BDMB, DMPA, BAPO and TPO) has been compared for use in thick photopolymerization systems illuminated with a standard mercury lamp and a high-intensity, 400 nm LED lamp. For each initiator/lamp combination, the spatial and temporal evolution of the photoinitiation rate profile was examined by numerically solving the set of governing differential equations. The simulation results revealed that, when illuminated by the Hg–Xe lamp, the photoinitiators BDMB or DMPA (which are efficient photoinitiators for thin coatings) were very ineffective for curing thick systems. In these cases, the photoinitiation rate is only significant at or near the surface, and competing absorption by the photolysis products does not allow light, and thus the initiation reaction, to extend more deeply into the sample. When illuminated with the Hg–Xe lamp, the photoinitiators BAPO and TPO exhibited effective photoinitiation for thick systems. Both of these initiators photobleach effectively in the major emission ranges of the lamp, allowing the photoinitiation reaction to extend into the depth of the sample. BAPO exhibits a higher molar absorptivity than TPO, which leads to higher photoinitiation rates and a sharper wave front propagating through the system.

The simulation results also revealed that, for some photoinitiators, the LED light source will be more effective than the Hg–Xe arc lamp for photopolymerization of thick systems. The LED lamp used in this study exhibited a 20 nm wide emission band centered around 400 nm. In this region of the spectrum, the BAPO and TPO photoinitiators exhibit more complete photobleaching, which leads to an increased maximum photoinitiation rate and enhanced progression of the photoinitiation profile through the sample. These results clearly illustrate that, in addition to the advantages of high energy efficiency, long lamp lifetime, low heat generation and the absence of hazardous vapors, LED light sources may also lead to more effective photoinitiation of thick polymer systems.

REFERENCES

1 Baikerikar KK and Scranton AB, *Polymer* **42**:431 (2001).
2 Baikerikar KK and Scranton AB, *J Appl Polym Sci* **81**:3449 (2001).
3 Coons LS, Rangarajan B, Godshall D and Scranton AB, *ACS Symp Ser* **673**:203 (1997).
4 Terrones G and Pearlstein AJ, *Macromolecules* **34**:3195 (2001).
5 Terrones G and Pearlstein AJ, *Macromolecules* **34**:8894 (2001).
6 Terrones G and Pearlstein AJ, *Macromolecules* **36**:6346 (2003).
7 Ivanov V and Decker C, *Polym Int* **50**:113 (2001).
8 Miller GA, Gou L, Narayanan V and Scranton AB, *J Polym Sci, Polym Chem Ed* **40**:793 (2002).
9 Stephenson N, Kriks D, El-Maazawi M and Scranton A, *Polym Int* **54**:1429 (2005).
10 Stephenson Kenning N, Kriks D, El-Maazawi M and Scranton A, *Polym Int* **55**:994 (2006).
11 Bala O, Olmez A and Kalayci S, *J Oral Rehabil* **32**:134 (2005).
12 Knezevic A, Tarle Z, Meniga A, Sutalo J and Pichler G, *J Oral Rehabil* **32**:362 (2005).
13 Teshima W, Nomura Y, Tanaka N, Urabe H, Okazaki M and Nanara Y, *Biomaterials* **24**:2097 (2003).
14 Odian G, *Principles of Polymerization*, 2nd edn. Wiley, New York (1981).
15 Goodner MD and Bowman CN, *Chem Eng Sci* **57**:887 (2002).
16 Perry MF and Young GW, *Macromol Theory Simul* **14**:26 (2005).

Polym Int **57**:1134–1140 (2008)
DOI: 10.1002/pi